The chronostratigraphic significance of seismic reflections along the Baham

5 AUTHORS, INCLUDING:

Gregor Eberli
University of Miami
101 PUBLICATIONS **1,187** CITATIONS
SEE PROFILE

Dick Kroon
The University of Edinburgh
176 PUBLICATIONS **4,810** CITATIONS
SEE PROFILE

James D Wright
Rutgers, The State University of New Jersey
129 PUBLICATIONS **4,773** CITATIONS
SEE PROFILE

ELSEVIER

Marine Geology 185 (2002) 1–17

MARINE GEOLOGY
INTERNATIONAL JOURNAL OF MARINE GEOLOGY, GEOCHEMISTRY AND GEOPHYSICS

www.elsevier.com/locate/margeo

The chronostratigraphic significance of seismic reflections along the Bahamas Transect

Gregor P. Eberli [a,*], Flavio S. Anselmetti [b], Dick Kroon [c], Tokiyuki Sato [d], James D. Wright [e]

[a] *University of Miami, Rosenstiel School of Marine and Atmospheric Science, 4600 Rickenbacker Causeway, Miami, FL 33149, USA*
[b] *Geological Institute, ETH, Sonneggstrasse 5, 8092 Zürich, Switzerland*
[c] *Department of Geology and Geophysics, University of Edinburgh, West Main Road, EH9 3JW Edinburgh, UK*
[d] *Institute of Applied Earth Science, Akita University, Tegata-Gakeuncho, Akita 010, Japan*
[e] *Department of Geological Sciences, Rutgers University, Piscataway, NJ 08854, USA*

Received 9 August 2000; accepted 20 September 2001

Abstract

Continuous cores drilled during the Bahamas Drilling Project (BDP) and the Ocean Drilling Program (ODP) Leg 166 along a transect from the top of Great Bahama Bank to the basin in the Straits of Florida provide a unique data set to test the assumption in seismic stratigraphy that seismic reflections are time lines and, thus, have a chronostratigraphic significance. Seismic reflections that are identified as seismic sequence boundaries (SSBs) were dated by means of biostratigraphy in the five ODP sites and by a combination of biostratigraphy, magnetostratigraphy and Sr isotope stratigraphy in the two BDP sites. The seismic reflection horizons are carried across a variety of facies belts from shallow-water carbonates over slope carbonates to drift deposits in the Straits of Florida. Within this system 17 SSBs were identified and dated. Despite the fact that the seismic reflections cross several facies belts, their ages remain remarkably constant. The average offset in all sites is 0.38 Myr. In no cases do the seismic reflections cut across time lines. The age differences are the combined result of the biostratigraphic sampling frequency, the spacing of marker species that required extrapolation of ages, and the resolution of the seismic data. In addition, uncertainties of age determination in the proximal sites where age-diagnostic fauna are rare add to the age differences between sites. Therefore, it can be concluded that the seismic reflections, which mark the SSBs along the Bahamas Transect, are time lines and can be used as stratigraphic markers.

This finding implies that depositional surfaces are preferentially imaged by reflected seismic waves and that an impedance contrast exists across these surfaces. Facies successions across the sequence boundaries indicate that the sequence boundaries coincide with the change of deposition from times of high to low sea level. In the carbonate setting of Great Bahama Bank, sea-level changes produce changes in sediment composition, sedimentation rate and diagenesis from the platform top to the basin. The combination of these factors generates differences in sonic velocity and, thus, in impedance that cause the seismic reflection. The impedance contrasts decrease from the proximal to the distal sites, which is reflected in the seismic data by a decrease of the seismic amplitude in the basinal area.

* Corresponding author.
E-mail address: geberi@rsmas.miami.edu (G.P. Eberli).

0025-3227/02/$ – see front matter
PII: S0025-3227(01)00287-0

Keywords: Bahamas; carbonates; chronostratigraphy; seismic sequence stratigraphy; sequence boundary; Bahamas Drilling Project; Ocean Drilling Program

1. Introduction

Seismic imaging has become a standard geophysical method to image the subsurface architecture of sedimentary basins (e.g. Watkins and Drake, 1982; Bally, 1983; Weimer and Davis, 1996). These subsurface images are caused by the physical interaction between seismic waves and the sediments and rocks. Nevertheless, stratigraphers postulated that stratigraphic information is also present on the seismic data and that the law of superposition is applicable to sedimentary packages seen on seismic sections (Payton, 1977). Furthermore, they began to use the seismic reflections as correlation lines, assuming that they followed depositional surfaces and erosional unconformities. This assumption that seismic reflections are time lines and carry a chronostratigraphic significance is the basis for seismic stratigraphy (Vail et al., 1977b). Seismic stratigraphy was refined with the advance of the seismic sequence stratigraphy concept, which postulated that each global sea-level change creates a characteristic sequence of sediments that can be correlated between sedimentary basins around the world (Vail et al., 1977a). By dating unconformities and flooding surfaces a global cycle chart was established by Vail et al. (1977a) and later refined by Haq et al. (1987). The sequence stratigraphic concept and its facies models have been controversial ever since they were proposed (Pitman and Golovchenko, 1983; Miall, 1986; Summerhayes, 1986; Cloetingh, 1986; Cathles and Hallam, 1991; Schlager, 1992). The controversies surrounding seismic sequence stratigraphy reflect two main problems. First, the difficulty in assessing the synchronicity of sea-level changes in different ocean basins, and second, the difficulty in separating the role of tectonic subsidence from eustasy in creating unconformity bounded sequences.

In the assessment of the timing and synchronicity of sea-level changes, the seismic sequence stratigraphy concept relies on the basic assumption that stratal surfaces, imaged by seismic reflections, are coincident with depositional surfaces and are essentially time lines (Vail et al., 1977b). High-resolution seismic data from the Equatorial Pacific were some of the first data sets in the public domain to corroborate this assumption (Mayer, 1979a,b; Mayer et al., 1986). However, several studies of seismic modeling showed that in some cases this precondition is not valid (Tipper, 1993; Stafleu and Sonnenfeld, 1994; Stafleu et al., 1994). These cases are either caused by extreme facies variations or by the limitation of seismic resolution (Rudolph et al., 1989).

To test the age consistency of seismic reflections assumption comprehensive data sets are needed that consist of good seismic data and sufficient core coverage along seismic lines. The seismic lines and the cores along the Bahamas Transect in combination with the precise time-to-depth conversion from the check-shot surveys provide such a long-awaited data set. The Bahamas Transect is located along the prograding margin of western Great Bahama Bank covering facies from the carbonate platform top to the pelagic sediments of the Straits of Florida (Eberli et al., 1997a; Anselmetti et al., 2000). Progradation occurred in pulses that are seen on the seismic lines as laterally stacked sequences. Geometries within these prograding sequences suggest that the pulses of progradation are sea level-controlled (Eberli and Ginsburg, 1987, 1989). Facies successions within seven cores retrieved along the transect during the Bahamas Drilling Project (BDP) and the Ocean Drilling Program (ODP) Leg 166 corroborate this seismic interpretation (Eberli et al., 1997a,b, 2001). In this paper, we elaborate on the test of chronostratigraphic significance of the seismic reflections and thus the seismic sequence stratigraphic concept for the investigated carbonate platform margin. Subsequently, we will discuss the physical causes for the chronostratigraphic significance of the reflections.

2. Data and results

2.1. The Bahamas Transect

The Bahamas Transect consists of the seismic image of western Great Bahama Bank, its margin and the adjacent basin in the Straits of Florida. The seismic lines image the platform basin system along approximately 150 km. Cores from seven sites cover a distance of 52 km from the platform top to the drift deposits in the Straits of Florida (Figs. 1 and 2). The facies of the transect range from shallow-water carbonates (Unda and Clino) to marginal reefs and periplatform ooze with variable amounts of redeposited deposits on the slope to pelagic deposits in the basin (Kievman, 1996, 1998; Kenter et al., 2001; Eberli et al., 1997a; Betzler et al., 1999; Swart et al., 2000). At the toe-of-slope site (ODP Site 1007) the base of the Neogene was reached. All other wells bottomed out at different levels in the Miocene, and at Site 1004 in the Pliocene.

On the platform top, cores from site Unda, 11.1 km away from the margin, recovered the

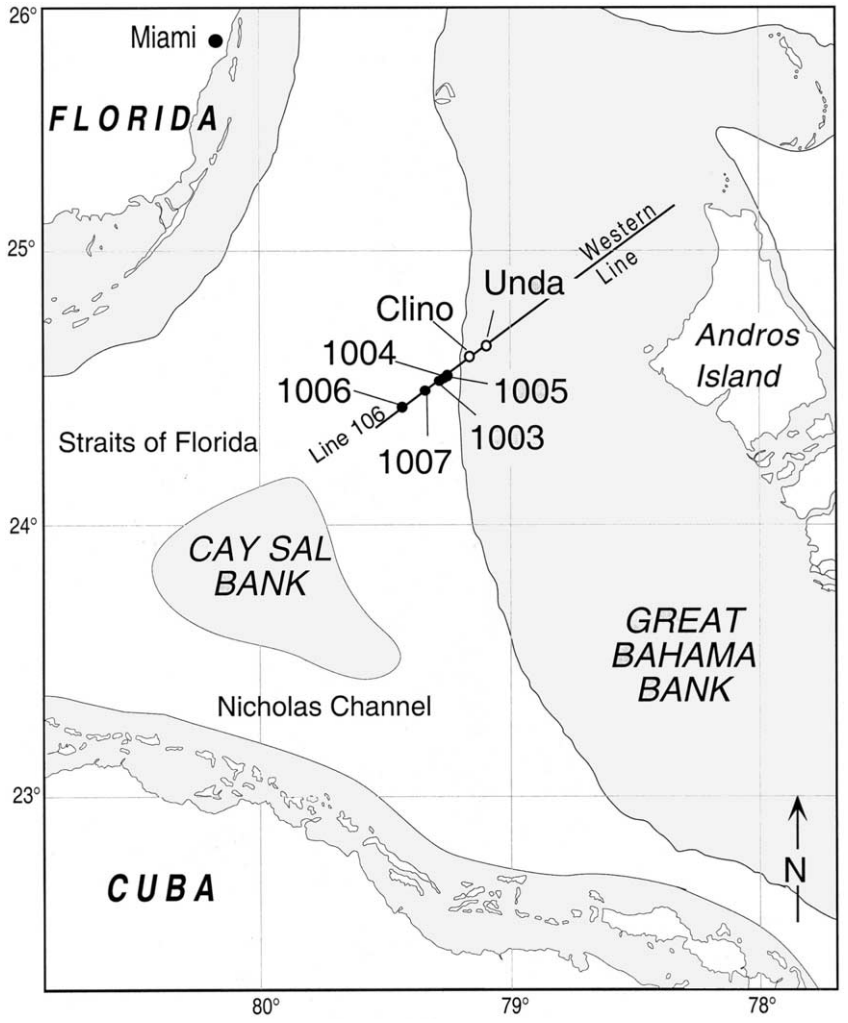

Fig. 1. Location map of the Bahamas Transect. The transect from Great Bahama Bank into the adjacent basin of the Straits of Florida is imaged by the Western Line in the platform interior and the seismic Line 106 in the basin. Cores from seven sites along the transect calibrate the facies and ages of the prograding margin.

interval of platform margin deposits in which sea-level falls are recorded by subaerial exposure horizons. Site Clino was positioned 3.6 km from the modern margin to penetrate a series of inclined reflections which image upper slope deposits underneath a thin, upper Pleistocene and Holocene platform succession. The drilling was performed from a self-propelled jack-up barge in approximately 7 m of water using conventional diamond drilling technology (Ginsburg, 2001). Core Clino was drilled 677.71 m below the mud pit datum (7.3 m, above sea level); recovery averaged 80.8%. Core Unda was drilled 454.15 m below the mud pit (5.2 m, above sea level) with an average recovery of 82.9% (Ginsburg, 2001). During ODP Leg 166, five sites (Sites 1003–1007) were drilled in the Straits of Florida, using the *Joides Resolution* as the drilling ship. Sites 1005, 1004, and 1003 are situated on the upper and middle slope and Site 1007 at the toe-of-slope. Site 1006 forms the distal end of the transect approximately 40 km away from the modern platform margin in the Straits of Florida. Core recovery in the ODP cores is 55.3% (Eberli et al., 1997a).

2.2. Seismic data

The seismic data along the transect consist of two vintages of seismic data. A long regional multi-channel seismic line acquired by Western Geophysical images the bank interior and the transition into the adjacent basin. It was acquired with a tuned array of airguns with a low-frequency band. In conjunction with the BDP, Exxon Production Research Company reprocessed part of the Western Line with a special emphasis on the top 2 s (twt). Resolution was improved by choosing higher-frequency bands during reprocessing. As part of the site survey for ODP Leg 166, a grid of high-resolution seismic lines was acquired in 1994 on board R/V *Lone Star* in collaboration with John Anderson and Andre Droxler from Rice University, Houston, TX, USA. A 24-channel streamer recorded the signal created by a 40-inch^3 GI-airgun. This system allowed a center signal frequency of 100–200 Hz that resulted in a seismic resolution of approximately 5–10 m. Seismic line 106 overlaps partially with the Western Line but extends farther into the Straits of Florida. The two data sets combined image the complete transition from the interior of the Great Bahama Bank into the Straits of Florida (Fig. 2).

By mapping reflection terminations and their related unconformities, a seismic sequence analysis was performed that yielded 17 Neogene to Quaternary seismic sequences (Eberli et al., 1997a). The geometric unconformities of the seismic sequence boundaries (SSBs), in particular in proximal positions of the platform, indicate that deposition of these sequences was strongly controlled by sea-level fluctuations that periodically exposed the platform top. This sea level-controlled sedimentation is confirmed with the lithology of the drilled cores (Eberli et al., 1997b, 2001; Anselmetti et al., 2000). All 17 SSBs can be carried out from the platform to the basinal section, where most of them are embedded in a conformable sedimentary package (Fig. 2). The distal areas in the Straits of Florida are characterized by current-influenced drift sedimentation. The drift deposits interfinger at the toe-of-slope with the slope deposits of the prograding margin (Anselmetti et al., 2000). Most SSBs cross this facies transition, which is indicated by a change in seismic facies from partly chaotic, caused by frequently incised slope deposits, towards highly coherent reflections of the current deposits.

2.3. Lithology

The two continuous cores Unda and Clino penetrate proximal portions of the prograding margin of Great Bahama Bank. Facies in core Unda consist of shallow-water and reefal deposits that alternate with sand to silt-sized deeper margin deposits. In the more distal core Clino, shallow-water deposits overlay a thick section of fine-grained slope deposits. Facies successions document changes in relative sea level. On the platform, SSBs coincide with surfaces of subaerial exposure, changes in facies and diagenetic overprints (Kievman, 1996). On the slope where the sediment consists of fine-grained skeletal and non-skeletal material, the sequence boundaries are marked by discontinuity surfaces that are either hardgrounds or cemented intervals overlain by

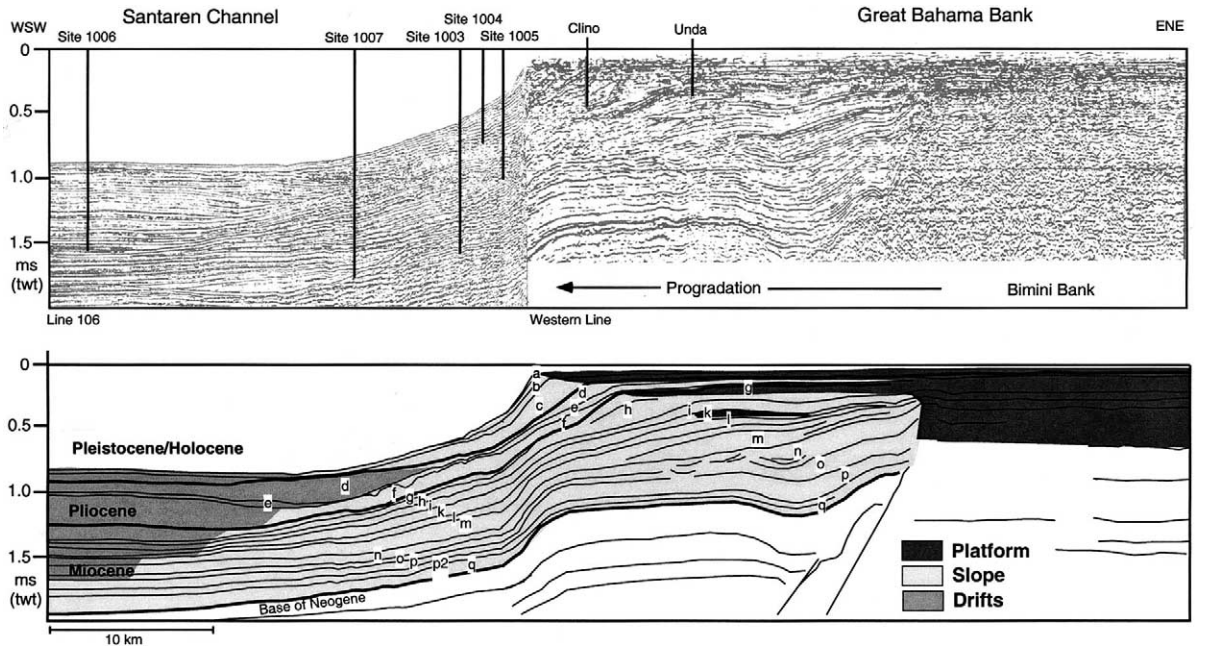

Fig. 2. Seismic cross-section across the western margin of Great Bahama Bank, displaying the 17 Neogene–Quaternary prograding sequences that are analyzed for age consistency. The cross-section consists of the high-frequency Line 106 in the offbank area and the lower-frequency Western Line across the platform top. Seismic sequences are labeled a–q; SSBs A-Q denominate the basal unconformities of the sequences (modified from Anselmetti et al., 2000).

coarser-grained intervals with blackened lithoclasts, planktonic foraminifera and minor amounts of platform-derived grains. The coarser-grained intervals are interpreted as deposits during relative sea-level lowstands and subsequent rises, while the fine-grained sediments are interpreted as highstand deposits (Kenter et al., 2001; Eberli et al., 1997b).

At the slope and basinal sites, compositional variations document an alternating pattern of bank flooding, concomitant shedding to the slope with periods of exposed banks, a shutdown of shallow-water carbonate production and largely pelagic sedimentation (Eberli et al., 1997a). These pulses of sedimentation produce the prograding clinoforms seen on seismic data (Fig. 2). At Site 1005, the most proximal site drilled on the upper slope during ODP Leg 166, a similar sedimentary succession consists of unlithified to partially lithified wackestones and slightly coarser-grained intervals consisting of packstones and grainstones. Few mass gravity flows are deposited in this proximal site, as most of the platform-derived turbidites bypassed the upper slope. In this upper slope setting, incisions are common, forming a series of canyons perpendicular to the platform edge (Anselmetti et al., 2000). Major incisions mark several SSBs, for example at the Miocene/Pliocene boundary and at the Early/Late Pliocene boundary. On the middle to lower slope (Site 1003) sedimentation is more variable. Sedimentary units consist either of fine-grained more neritic sediments, pelagic deposits, or turbidite successions. Channels and incisions are more abundant but of smaller dimension (Betzler et al., 1999). Except for the last 700 kyr, the toe-of-slope (Site 1007) is the main depositional location for redeposited carbonates which accumulate during both sea-level highstand and sea-level lowstands (Betzler et al., 1999; Bernet et al., 2000; Rendle and Reijmer, 2002). The turbidite lenses are discontinuous within the marl/limestone alternations that form the background sedimentation. The distal portion of the sequences is dominated by cyclic marl/limestone alternations with few turbidites. In addition, drift deposits dominate the basinal sediments

Table 1
Biostratigraphic datums and their occurrence with depth in the ODP sites and Unda and Clino

Event	Nanno-fossil age (Ma)	Foram-inifer age (Ma)	Site 1006 depth (mbsf)	Site 1007 depth (mbsf)	Site 1003 depth (mbsf)	Site 1004 depth (mbsf)	Site 1005 depth (mbsf)	Site Clino depth (mbmp)	Site Unda depth (mbmp)
B *E. huxleyi*	0.25		4.24		14.14	19.43	20.49		
T *P. lacunosa*	0.41		20.53		57.23	38.56	69.6	< 184.45	< 110.06
T *R. asanoi*	0.85		39.53		86.46	81.16	126.56		
T *Gephyrocapsa* spp. (lg)	1.2		48.49	14.23	96.98		172.74		
B *Gephyrocapsa* spp. (lg)	1.44		68.03	31.67			182.88		
B *G. caribbeanica*	1.72		91.78	43.54	113.19	152.03	190.49		
T *G. extremus*		1.77	88.2	53.54	109.05			204.36	196.64
B *Gr. truncatulinoides*		2	97.69	53.54	123.75			378.80	
B *Gr. exilis*		2.2	107.18	53.54	132.7			268.3 NR	
T *Gr. miocenica*		2.3	116.8		132.7			507.31	234.75
T *Gr. limbata*		2.3	135.36	53.54	132.70	186.41			
T *G. pertenius*		2.6				186.43	203.45	510.97	
T *D. altispira*		3.1	145.22	200.34	142.90		226.72		
B *G. miocenica*		3.55	173.25					532.01	235.97
T *G. margaritae*		3.58	173.25	200.34	159.33			532.01	
T *R. pseudoumbilica*	3.6		172.53	200.34	155.79		247.52	NR	263.11
T *G. nepenthes*		4.2	240.28	200.34	197.98		274.1	541.46	
B *Ceratolithus rugosus*	4.7		325.98	287.61			365		
T *D. quinqueramus*	5.6		383.42						
B *Globigerinoides conglobatus*		6.2	436.04	327.87	355.61		415.98	553.30	288.06
B *Gr. cibaoensis*		7.7	483.07	327.87	355.61		415.98		
B *Gs. extremus*		8.1	492.05	327.87	355.61		415.98	NR	
T *D. neohamatus*	8.7		500.95	327.99	359.01		415.98	585.06	
T *D. hamatus*	9.4		530.48	432.99	488.75		495.28	635.06	
B *D. hamatus*	10.7		567.45	481.68	531.60		582.35	672.76[a]	
B *C. coalitus*	11.3		602.51	503.69	555.10		595.78		
T *Gr. mayeri*		11.4	595.39	481.69	561.04		595.78		
B *G. nepenthes*		11.8	625.08	532.75	630.52		651.82	672.76*	
T *Fohsella* spp.		11.9	639.96	542.48	641.30		670.90		
B *F. fohsi*		12.7	682.02	742.12	802.55				NR
T *C. floridanus*	13.2		696.27	769.40	780.00				
T *S. heteromorphus*	13.6			780.59	856.84				
B *F. praefoshi*		14		791.54	910.76				
T *P. sicana*		14.8		800.20	910.76				
B *O. universa*		15.1		808.39	910.76				
T *H. altiaperta*	15.6			857.50	1058.06				
B *P. sicana*		16.4		910.25	1089.72				
T *C. dissimilis*		17.3		925.35	1089.72				
T *S. belemnos*	18.3			967.44	1108.08				
B *Ge. insueta*		18.8		973.41	1140.00				
B *S. belemnos*	19.2			1003.04	1171.86				
B *Gs. altiapertura*		20.5		1086.75	1204.13				
T *Gr. kugleri*		21.5		1099.62	1204.13				
B *D. druggi*	23.2			1117.85	1242.52				

The lack of Pleistocene datums in the proximal sites Unda and Clino is due to the progradation of shallow-water carbonates that are barren of planktic fossils. NR = not reliable in regard to the depth of occurrence (Lidz and Brawlower, 1994; Lidz and McNeill, 1995a).

[a] Depth of first sample in Clino. Depths for Unda and Clino are reported as meters below mud pit. For Clino, sea level was 7.3 m below the mud pit and the sea floor was 14.9 m; for Unda, sea level was 5.2 m below the mud pit and the sea floor was 11.9 m. Data for the ODP sites from Leg 166 shipboard party (1997) and Wright and Kroon (2000).

from the late Middle Miocene onward (12.4 Myr) at the Bahamas Transect.

2.4. Biostratigraphy

The biostratigraphic data form the basis of age dating of the seismic reflections identified as sequence boundaries (Table 1). At Site 1006, located in the most distal position from the platform in the Straits of Florida, the most conventional nannofossil and planktonic foraminiferal biohorizons were found in the Pleistocene to Middle Miocene (Eberli et al., 1997a; Kroon et al., 2000, Wright and Kroon, 2000). Towards the platform and with depth, the microfossils showed a progression from well preserved to poorly preserved specimens. In all sites, the zonal scheme of Blow (1969), with slight modifications by Kennett and Srinivasan (1983) and Curry et al. (1995), was used to subdivide the Neogene into planktonic foraminiferal zones. Age estimates for the Cenozoic datum levels are taken from Berggren et al. (1995a,b), except for the first occurrence of *Globigerinoides conglobatus* at 6.2 Myr (Chaisson and Pearson, 1997). Ship- and shore-based analysis of planktonic foraminifera from thin clay-rich layers with little diagenetic alterations yielded a robust planktonic biostratigraphic framework at the ODP site (Wright and Kroon, 2000). Further refinement of the ages is

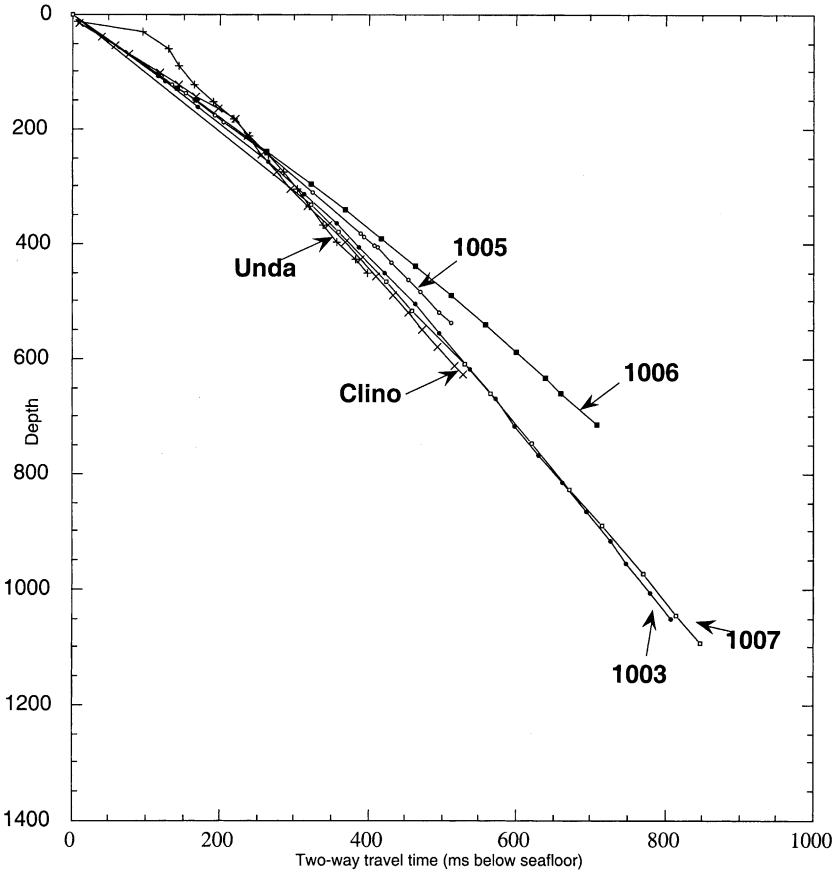

Fig. 3. Travel time-to-depth correlation curves obtained from check-shot experiments in the ODP drillsites and the banktop sites Unda and Clino. These well seismic data correlate accurately the depth of the seismic reflections in two-way travel time (ms) to the depth (m) in the cores. For Site 1004, where no check-shot data are available, the shallow portion of the correlation curve of the other sites was used.

expected by using the eccentricity cycles observed on logs of Site 1006 in combination with the biostratigraphy for the construction of the age model. This method will potentially allow dating the sediments and reflections with a precision of two eccentricity cycles, i.e. 200 kyr (Williams et al. 2002).

In the proximal sites Unda and Clino biostratigraphic dating was extremely difficult, mainly as a result of the absence of sufficient age-diagnostic shallow-water fossils, lack of open-ocean biostratigraphic markers, and relatively early and pervasive diagenetic alteration. Nevertheless, benthic and planktonic foraminifera and calcareous nannofossils were recovered throughout Unda and Clino (Lidz and Brawlower, 1994; Lidz and McNeill, 1995a). In these proximal sites, there was originally no entirely straightforward age interpretation for either hole (Lidz and Brawlower, 1994). Resampling of thin units of pelagic-rich sediment, deposited during times when platform sediment supply was greatly reduced, resulted in a refinement of the biostratigraphic age model for these two holes (Lidz and McNeill, 1995a). In both analyses the late Neogene foraminiferal zonation of Bolli and Saunders (1985) and the nannofossil zonation of Martini (1971) were adapted to the time scale of Berggren et al. (1985). These data were then adapted for the Berggren et al. (1995) time scale to date the seismic reflections in this proximal portion of the transect in a consistent manner with the distal sites (McNeill et al.,

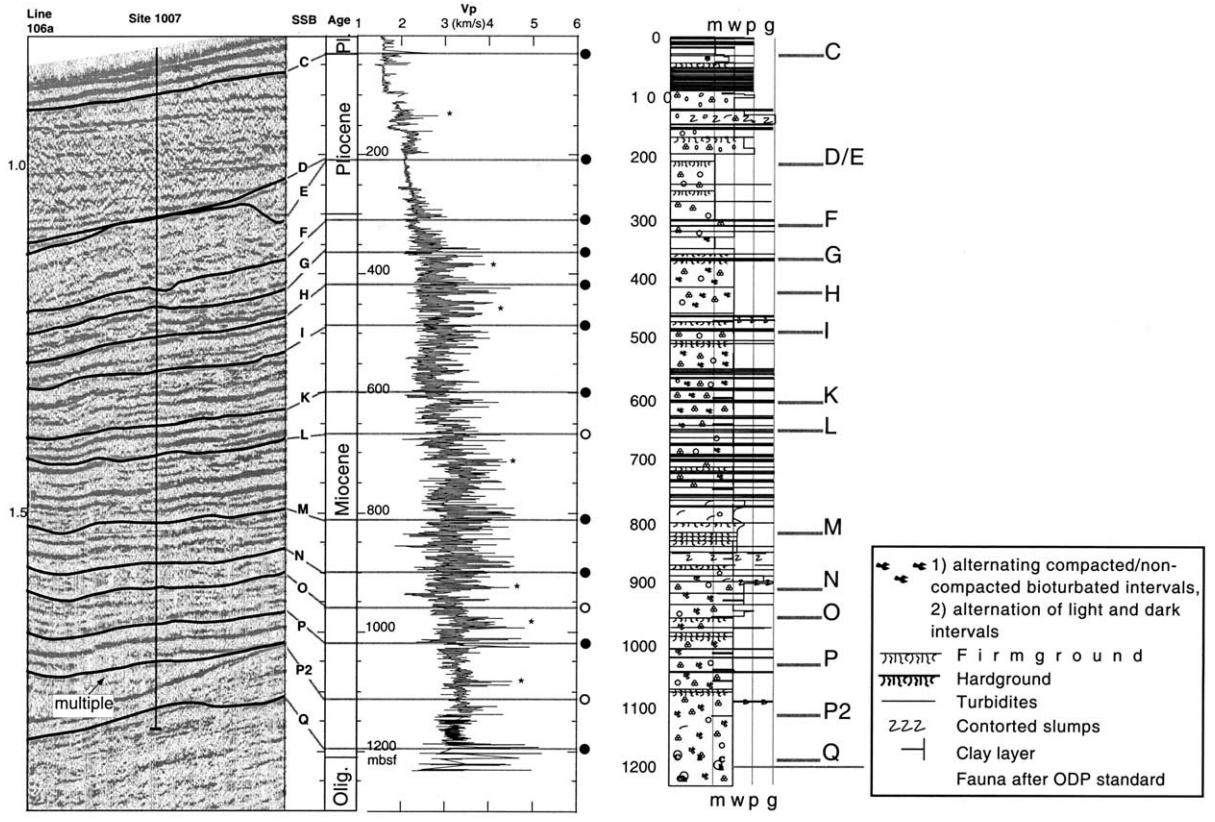

Fig. 4. Seismic section with SSBs at ODP Site 1007 and the correlation to the sonic and lithologic log. Most SSBs coincide with distinct changes in the log (marked by solid circles on the side). Lithologic changes across boundaries include increase of turbidites, hardgrounds and firmgrounds, which cause changes in the sonic velocity. The variations in velocity are controlled by lithological changes but also by diagenetic alteration. Erosional unconformities are recognized on the seismic data in the Pliocene interval, while in the Miocene section sequence boundaries are conformable (modified from Anselmetti et al., 2000; lithology from Bernet et al., 2000).

2001). In Table 1, only the marker species of Unda and Clino that are also present in the distal sites are listed. A large number of other foraminifera and nannofossils were, however, used in combination with strontium isotope stratigraphy and magnetostratigraphy to provide an age model for the platform sites (Lidz and McNeill, 1995a; Swart et al., 2001; McNeill et al., 2001).

2.5. Time–depth conversion

Seismic reflection events are recorded in two-way travel times. These times have to be converted into depth units so that they can be tied to the cores. Several methods allow an estimation of the distribution of seismic velocity that controls a time–depth conversion (i.e. sonic log velocities or stacking velocities). Precise correlation, however, for a high-resolution seismic survey as along the Bahamas Transect can only be achieved by performing a check-shot survey in the drillhole after completion of drilling operations. For this purpose, a single-channel well seismic tool was used at various depths in the drillholes to record the travel time of a downgoing acoustic signal from an airgun that was fired next to the drill ship or the jack-up platform. A check-shot survey was performed at all drillsites except Site 1004, which penetrated only 200 m and for which the average shallow portion of the curves of the other offbank sites is used. The resulting time-to-depth conversion curves vary significantly between the individual drillsites (Fig. 3), and document lateral variation in the distribution of physical properties.

The following procedure is used to determine the age of reflections that are identified as SSBs: (1) the two-way travel time is measured from the center of the sea floor reflection to the center of the reflection defining the SSB. (2) Using the interpolated time–depth curve from the first-arrival data of the check-shot survey (Fig. 3), the sub-bottom travel time is converted to depth in meters below sea floor. (3) All biostratigraphic data are plotted in a depth–age graph, so that a best-fit curve can be defined through the data points representing the most likely depositional history of the cores (Eberli et al., 1997a). Gaps between two age markers are covered with a linear extrapolation, which does not consider small-scale fluctuations in sedimentation rate. (4) This best-fit curve is used to assign ages to the converted depths of the SSBs. In the case that a seismic reflection lies close to a biostratigraphically detected hiatus, the assigned age of the reflection will be the time span of the hiatus. Fig. 5 gives an example of the position of the sequence boundaries in the age–depth plot of Site 1007. (5) Finally, an estimated age of each SSB is determined. The age in the conformable portion of the sequence is given more weight since, in some cases, erosional down-cutting on the slope yields slightly older ages of the SSB in the proximal areas compared with the ages in the distal areas (Table 2).

The comparison of the seismic interpretation with biostratigraphic core data allows for a test of the seismic sequence stratigraphic concept for the investigated carbonate platform margin setting. Site 1007 is at the toe-of-slope where the Pliocene sequence boundaries are unconformities while the Miocene boundaries are conformable (Fig. 4). SSBs D and E merge on the seismic image due to a down-cutting erosion at the base of Sequence *d*. Biostratigraphically this erosion is recognized as a hiatus (Fig. 5). Similarly a slight erosion occurs on top of Sequences *g* and *d*, producing a hiatus at the respective sequence boundary. These hiatuses correlate with exposure horizons at the proximal sites Unda and Clino (Table 3, Fig. 6). The missing sequence *b* and the very thin sequence *a* (1.82 m; Rendle and Reijmer, 2002) are present on the platform top and both sequence boundaries show signs of exposure. The major erosion that leads to the merging of D and E at site 1007 is also recognized in Clino but did not remove the entire sequence. The major hiatus at the Mio–Pliocene boundary (SSB F) is expressed in Unda by an exposure surface/hardground on top of a marginal reef (Fig. 6). At Clino, the same sequence boundary is formed by a phosphatic crust and a hiatus of at least 1.3 Myr duration. This correlation indicates that sea-level falls produce subaerial exposure on the banktop, and hardground formation or erosion on the slope.

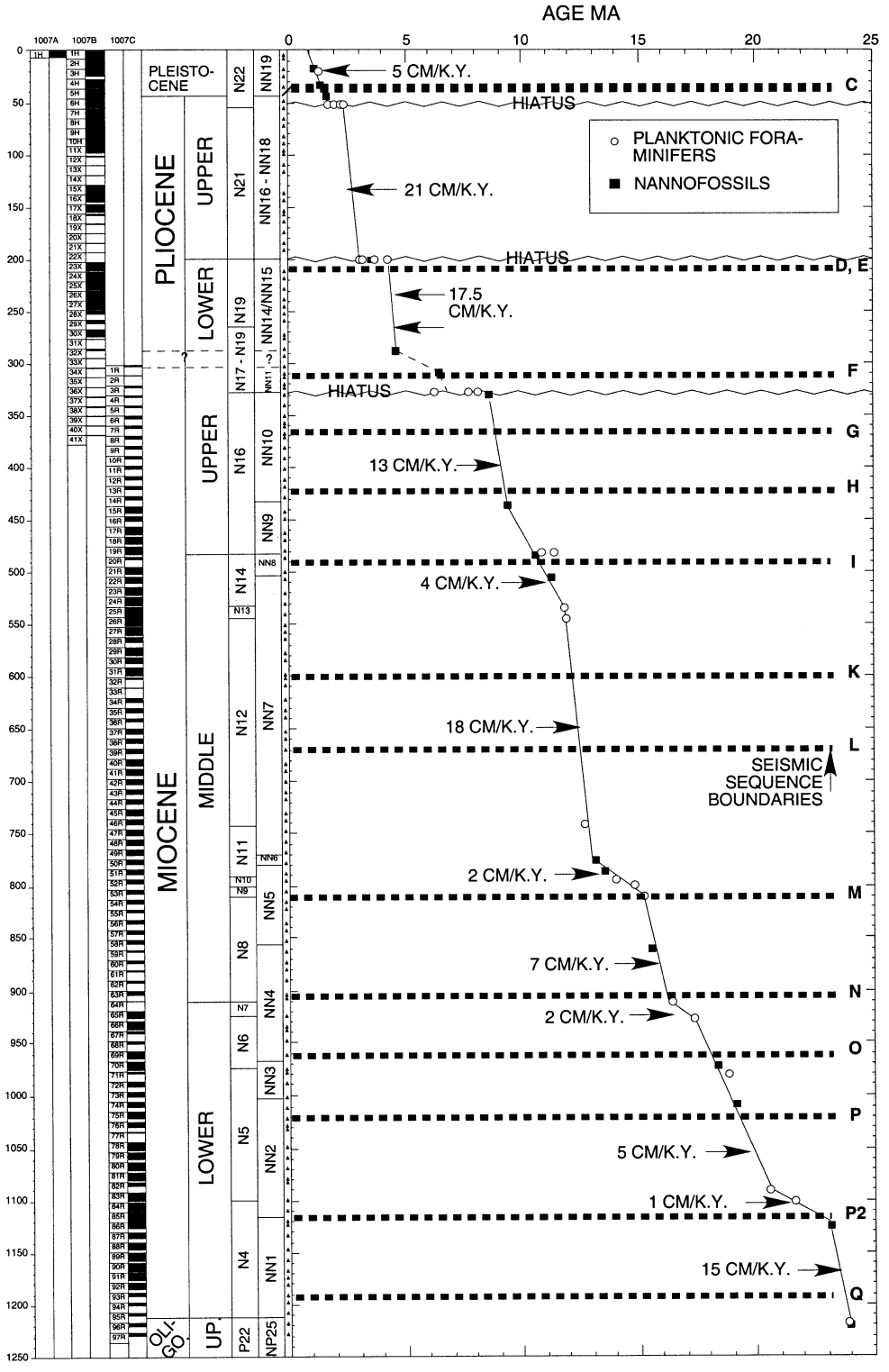
AGE MA
0
5
10
15
20
25
1007A
1007B
1007C
PLEISTO-CENE
PLIOCENE
MIOCENE
UPPER
LOWER
MIDDLE
OLIGO.
UP.
N22
N21
N19
N17 - N19
N16
N14
N13
N12
N11
N10
N9
N8
N7
N6
N5
N4
P22
NN19
NN16 - NN18
NN14/NN15
NN11
NN10
NN9
NN8
NN7
NN6
NN5
NN4
NN3
NN2
NN1
NP25
5 CM/K.Y.
HIATUS
21 CM/K.Y.
HIATUS
17.5 CM/K.Y.
HIATUS
13 CM/K.Y.
4 CM/K.Y.
18 CM/K.Y.
2 CM/K.Y.
7 CM/K.Y.
2 CM/K.Y.
5 CM/K.Y.
1 CM/K.Y.
15 CM/K.Y.
PLANKTONIC FORA-MINIFERS
NANNOFOSSILS
SEISMIC SEQUENCE BOUNDARIES
C
D, E
F
G
H
I
K
L
M
N
O
P
P2
Q

Fig. 5. Age–depth plot with sedimentation rates derived from biostratigraphic dating with the position of the SSBs at Site 1007. SSBs that are recognized as unconformities on Fig. 4 are detected biostratigraphically by a hiatus. Several sequence boundaries coincide with decreased sedimentation rates, indicating formation during times of reduced platform production and lowered sea level (modified from Eberli et al., 1997a).

Sedimentation rates vary throughout the Miocene–Pliocene section. For example at ODP site 1007, high sedimentation rates up to 21 cm/kyr correlate to sediments with fine and coarse material from the adjacent platforms (Fig. 5). In intervals with reduced sedimentation rates of approximately 2 cm/kyr sediments are dominated by pelagic microfossils (Eberli et al., 1997a). This variation in platform-derived material indicates changes of sea level. Platform exposures during sea-level lowstands are reflected in reduced sedimentation rates and mostly pelagic deposition. These intervals of reduced sedimentation coincide with several sequence boundaries (Fig. 5). Subsequent sea-level rise and flooding of the platform re-initiated carbonate production and shedding of neritic components to the slopes of the platform.

2.6. Chronostratigraphic ages of SSBs across transect

Although the above described procedure carries the uncertainty of both the exact position of the biostratigraphic datums and the seismic resolution, the sequence boundaries showed consistent ages along the seismic reflections. Table 2 displays the calculated estimated age and the maximum differences of each SSB across the transect based on the biostratigraphic information assembled on board *Joides Resolution* during Leg 166 (Eberli et al., 1997a) and refined in post-cruise research (Kroon et al., 2000; Wright and Kroon, 2000). The differences in age from site to site lie all between 0 and 0.9 Myr with an average variation of 0.38 Myr (Table 2). The fluctuations of the ages

Table 2
Ages of SSBs along the Bahamas Transect at each site and the estimated age of each SSB

SSB	Site 1006	Site 1007	Site 1003	Site 1004	Site 1005	Clino	Unda	Estimated age	Maximal offset
A	ND	ND	0.09	0.16	0.1	<0.83		0.1	0.07
B	ND	ND	0.25	0.73	0.6	<0.83	<0.83	0.6	0.25
C	1.8	1.5–1.7	1.2–1.6	1.7	1.6	1.9–2.1	1.9–2.0	1.7	0.4
D	3.1	3.2–4.2[a]	3.1	2.6	2.9	3.0–2.2[a]	$\sim$2.2 Ma	3.1	0.9
E	3.6	3.2–4.2	3.8		3.6	3.5–3.6	3.5–3.6	3.6	0.2
F	5.4	5.5–6.4[a]	5.6		6	$\sim$5.3–4[a]	$\sim$5.2–4.2[a]	5.4	0.6
G	8.7	8.8	6.2–8.7		6.2–8.8		7.9–5.9[a]	8.7	0.8
H	9.4	9.4	9		9.3		8.9–10.4[b]	9.4	0.4
I	10.7	10.9	10.6		10.2			10.7	0.7
K	12.4	12.2	12.2					12.2	0.2
L	12.7	12.5	12.7					12.7	0.2
M		15.1	13.6–15.1					15.1	0.0
N		16.2–16.4	15.9					15.9	0.3
O		18.2	18.4					18.3	0.2
P		19.4	19.2					19.4	0.2
P2		23.2	19.4–22.5					23.2	0.7
Q		23.7						23.7	–
									average Δt: 0.38

The maximal offset in Myr from the estimated age is given in the last column. Thicknesses of seismic sequences *a* and *b* are below seismic resolution at Sites 1006 and 1007 but sediments of Pleistocene–Holocene age are present at these locations (Rendle et al., 2000; Rendle and Reijmer, 2002). Ages in Myr. ND = not detectable.

[a] Hiatus, age range gives minimum duration of hiatus.

[b] Age uncertain.

of any of the SSBs along the seismic line 106, i.e. the ODP sites, are lower, i.e. 0.32 Myr (Anselmetti et al., 2000). This increased consistency of the ages in this portion reflects the better biostratigraphic dating in the slope and basinal areas. Assuming an approximate sedimentation rate of 5 cm/kyr, as determined as overall rate at Site 1007, the average error of 0.32 Myr equals a sediment thickness of 16 m. These values lie within the limitations of both seismic or biostratigraphic resolution. The average accuracy in determining the depth of a SSB amounts to approximately 10–20 m, which includes the uncertainty of picking the reflection and measuring the travel time, but not a wrong seismic interpretation, e.g. picking a different reflection. The errors of biostratigraphy are more difficult to assess, since the accuracy is related to factors such as sample selection, late first and premature last occurrences of marker species and reworking or mixing of older fauna (Lidz and McNeill, 1995b). It is, however, remarkable that all Neogene seismic horizons can be traced from the drift deposits in the Straits of Florida to the platform interior of Great Bahama Bank with an age error that originates from the basic seismic and biostratigraphic resolution and not from an incorrect seismic correlation. Even the drift deposits maintain their biostratigraphic integrity despite the fact that ocean currents reworked them. Thus, the ages of the seismic reflections along the Bahamas Transect are in fact time lines with chronostratigraphic significance. They document that, in this case, seismic reflections, and in particular the SSBs, do not cross cut time lines and can be used to perform a sequence stratigraphic analysis.

3. Discussion

The fact that the seismic reflections correlate across the depositional facies transitions and boundaries without changing their chronostratigraphic positions implies that the seismic reflections image the depositional surface rather than lithologic facies. It further implies that an impedance contrast is generated along the entire platform margin transect. Physically impedance (the product of velocity and density) controls the acoustic behavior of a medium. In platform carbonate settings velocity is the dominant factor controlling impedance (Anselmetti et al., 1997). Sonic velocity in carbonates is controlled by the combined effect of depositional lithology and diagenetic overprint (Anselmetti and Eberli, 1993, 1997). In order to create impedance changes along the entire transect, either the lithology and/or diagenesis need to change along the entire transect.

The investigated seismic reflections are sequence boundaries that represent a fall of sea level that dramatically changes the sedimentation and diagenesis in a platform margin setting. Carbonate platforms are most productive when they are flooded during high sea level. During these times they export abundant aragonite sediment to the slopes (Boardman and Neumann, 1984; Droxler et al., 1983; Droxler and Schlager, 1985; Reijmer et al., 1988; Wilber et al., 1990; Glaser and Drox-

Table 3
Ages of hiatuses caused by erosion at Site 1007 and their time-equivalent facies expression in the platform sites Clino and Unda

SSB	Site 1007 Toe-of-slope	Clino Platform margin	Unda Platform interior
A	hiatus isotope stage s 2-17	exposure surface	NP
B	merged with SSB A	discontinuity/exposure horizon	exposure horizon
C	erosional unconformity 1.5–1.7[a]	base of reef	firmground
D	erosion	erosional contact	discontinuity within stacked reef
E	erosional unconformity 3.2–4.2[a]	base of interruption	base of reworked skeletal packstone
F	erosional unconformity 5.5–6.4[a]	hardground, phosphatic crust	exposure horizon on reef, hardground
G	8.8	not reached, below TD	discontinuity surface

The erosional events correlate to exposure horizons, their coeval hardgrounds on the slope or bases of reworked upper slope material. Ages in Myr. NP = not present.

[a] Hiatus, age range gives minimum duration of hiatus.

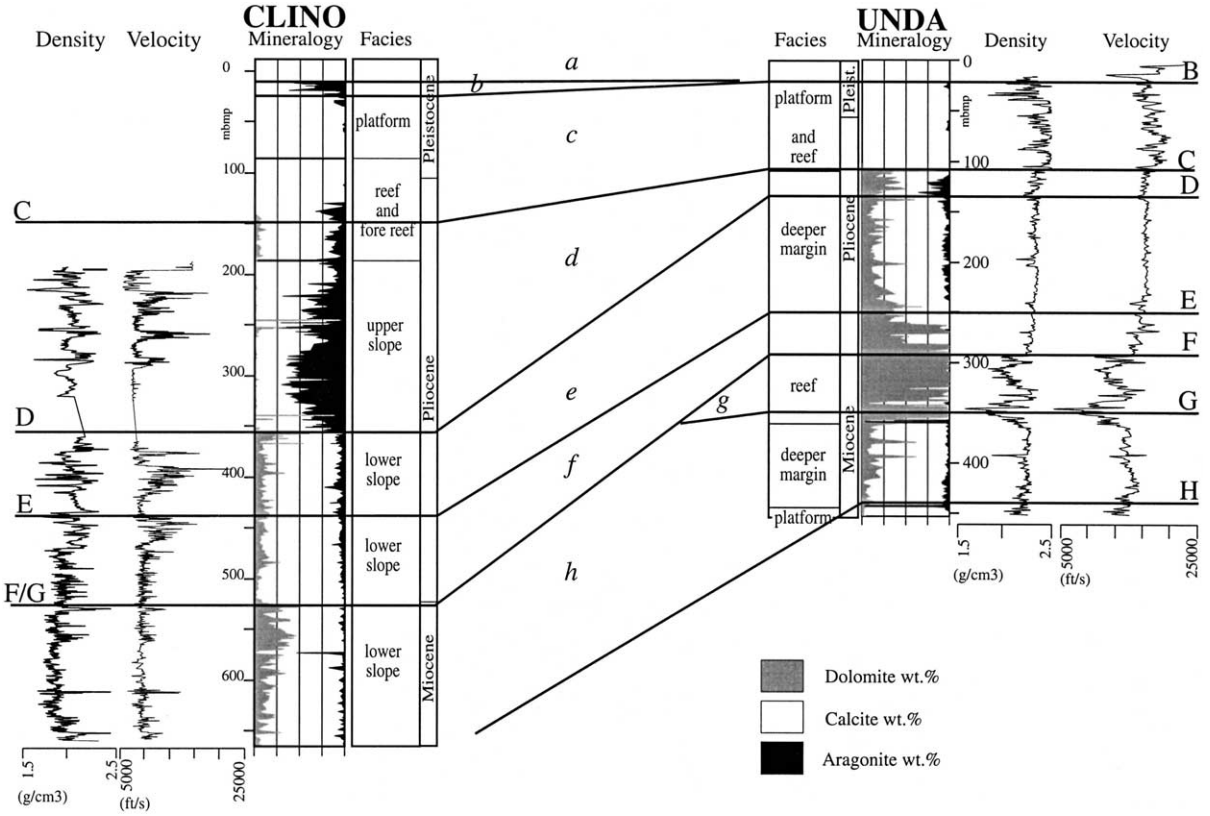

Fig. 6. Correlation between SSBs, sonic velocity, density and mineralogy and facies at the proximal sites of the transect at Unda and Clino. Many SSBs coincide with changes in mineralogy. In the slope site Clino, an increased amount of dolomite below SSBs is observed that is also reflected in increased sonic velocity. In the rather uniform slope sediments of Clino diagenetic variations largely control the distribution of velocity.

Table 4
Facies and velocity distribution across sequence boundary F (Miocene/Pliocene) along the transect

SSB F	Site 1006	Site 1007	Site 1003	Site 1005	Clino	Unda
Facies above SSB F	nannofossil ooze with firmgrounds	scour surface overlain by turbidites	wackestones to mudstones light gray	wackestone	coarse-grained skeletal non-skeletal pack–grainstone	sucrosic dolomite
Velocity (km/s)	2.0	2.1	2.1	2.2	2.6	2.5
Facies below SSB	nannofossil ooze with firmgrounds	foraminifer wackestone, nannofossil chalk	wackestones to mudstones brownish gray	wackestone with increased amount of insoluble residue	phosphatic hardground on fine-grained wackestone	dolomitized reef
Velocity (km/s)	2.1	2.0	2.3	2.6	2.8	3.7

At all sites a change in velocity occurs across the boundary. Facies changes are strong in the proximal sites and at the toe-of-slope site 1007, while they are subtle or missing in the other slope and basinal sites. For discussion see text.

ler, 1991; Grammer et al., 1993; Schlager et al., 1994). During sea-level lowstands platform production is reduced and the amount of pelagic deposition of predominantly calcitic marine microfossils increases. These mineralogical changes produce a difference in the diagenetic potential of the slope deposits (Frank and Bernet, 2000). Petrophysical variations due to this process can be measured on the slopes and in the basins surrounding the Bahamas (Eberli, 1988; Eberli et al., 1997a). Grammer et al. (1993), Westphal (1998) and Westphal et al. (1999) have documented how these changes in composition result in alternations of well cemented and less cemented intervals on the platform margin and uppermost slope.

Table 4 lists the facies and sonic velocity (determined from logs and check-shot) across SSB F, the Miocene/Pliocene boundary that was penetrated at six sites. The sonic velocity of the immediate overlying strata is in all sites, except at site 1007, lower than below sequence boundary. This difference is most dramatic in the most proximal site Unda where a subaerially exposed and dolomitized reef is overlain by fine-grained sucrosic dolomite (Fig. 6). The velocity contrast decreases towards the basin as a result of diminishing facies and diagenetic contrast. In three cases the facies vary significantly across the boundary, in the other three cases no distinct facies change occurs (Table 4). However, small changes in the sediment composition and grain size in the periplatform ooze and the interbedded redeposited beds can be detected in all sites (Bernet et al., 2000; Rendle et al., 2000; Kenter et al., 2001). Diagenetic boundaries coincide with the sequence boundaries in the platform sites Unda and Clino (Eberli et al., 2001) and small changes in diagenetic overprint are seen in the slope sites (Melim, personal communication). Kramer et al. (2000) document an increased dolomite content in the slope sites that can be related to SSBs. Reasons for the changes in composition and diagenesis are the sedimentary and hydrological processes related to sea-level changes. Fig. 7 displays a schematic overview of the process creating impedance contrasts along a platform basin transect. The aragonite-rich highstand sediments are altered at the sea floor and in the marine phreatic realm to create dense strata of higher velocity. The overlaying lowstand deposits are generally diagenetically less altered and have lower sonic velocity (Frank and Bernet, 2000). In addition, a small

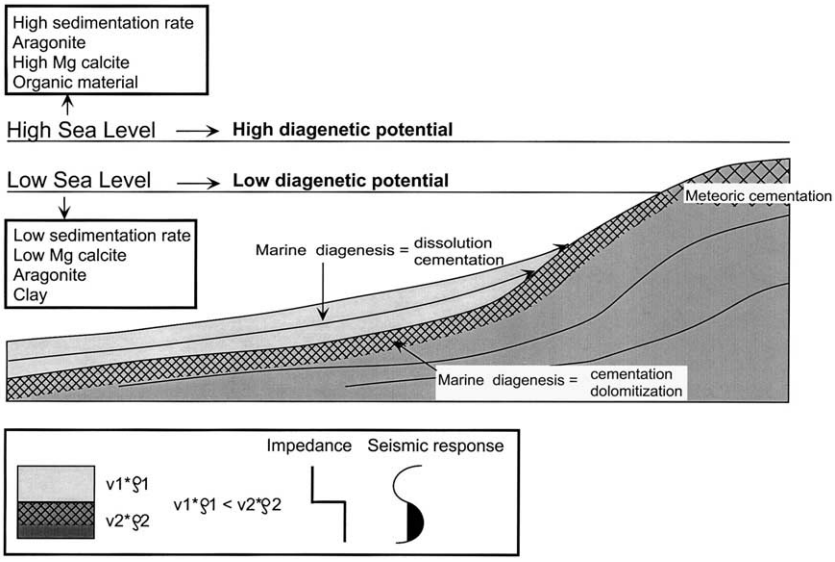

Fig. 7. Schematic display of impedance contrasts along sequence boundaries in carbonate platform margin settings. The juxtaposition of sediments with different composition and diagenetic potential during sea-level highstands versus lowstands results in density and velocity variations that create the necessary impedance in each facies belt.

admixture of siliciclastic material often occurs during sea-level lowstands in the slope and basin and a small grain difference between highstand and lowstand deposits is present along all the slope sites (Rendle et al., 2000). The siliciclastic admixtures reduce further the sonic velocity in the lowstand packages (Kenter et al., 2001). In summary, differences of facies and diagenesis occur in all facies belts along the transect. They are responsible for the acoustic differences and the impedance contrasts that cause seismic reflections along depositional surfaces, thereby giving them a chronostratigraphic significance.

4. Conclusions

The seismic lines and cores along the Bahamas Transect have confirmed one of the main assumptions in seismic sequence stratigraphy that seismic reflections have chronostratigraphic significance. This interpretation is based on the fact that ages of seismic reflections remained consistent along the transect, despite the fact that they crossed several facies boundaries. The reason for this age consistency of reflections is the fact that sedimentary and diagenetic changes are occurring simultaneously along the transect. The driving mechanism behind these changes is a fluctuating sea level that causes changes in sediment composition and diagenetic overprint. These two parameters influence the petrophysical behavior of the strata and cause surface-related impedance contrasts.

Acknowledgements

The scientific participants of BDP, the seismic survey and ODP Leg 166 contributed all to the data presented in this paper. We thank all of them for their input. These various endeavors were supported by NSF Grants OCE-8917295, OCE-9204294, OCE-9314586, and DOE Grant DE-FG05-92ER14253, JOI-USSAC Grant 166F000330, and the Industrial Associates of the Comparative Sedimentology Laboratory. The careful reviews of Christian Betzler and John Reijmer improved the manuscript.

References

Anselmetti, F.S., Eberli, G.P., 1993. Controls on sonic velocity in carbonate rocks. In: Liebermann, R.C. (Ed.), PAGEOH: Pure and Applied Geophysics 141, 287–323.

Anselmetti, F.S., Eberli, G.P., 1997. Sonic velocity in carbonate sediments and rocks. In: Marfurt, F.J., Palaz, A. (Eds.), Carbonate Seismology: Society of Exploration Geologists. Geophysical Developments Series 6, pp. 53–74.

Anselmetti, F.S., Eberli, G.P., Bernoulli, D., 1997. Seismic modeling of a carbonate platform margin (Montagna della Maiella, Italy): variations in seismic facies and implications for sequence stratigraphy. In: Marfurt, F.J., Palaz, A. (Eds.), Carbonate Seismology: Society of Exploration Geologists. Geophysical Developments Series 6, pp. 373–406.

Anselmetti, F.S., Eberli, G.P., Zan-Dong, D., 2000. From the Great Bahama Bank into the Straits of Florida: A margin architecture controlled by sea level fluctuations and ocean currents. Geol. Soc. Am. Bull. 112, 829–846.

Bally, A.W., 1983. Seismic Expression of Structural Styles – a picture and work atlas. American Association of Petroleum Geologists Studies in Geology Series 15, vol. 1–3.

Berggren, W.A., Hilgen, F.J., Langereis, C.G., Kent, D.V., Obradovich, J.D., Raffi, I., Raymo, M.E., Shackelton, N.J., 1995a. Late Neogene chronology: new prospective in high-resolution stratigraphy. GSA Bull. 107, 1272–1287.

Berggren, W.A., Kent, D.V., Flynn, J.J., Van Couvering, J.A., 1985. Cenozoic geochronology. Geol. Soc. Am. Bull. 96, 1407–1418.

Berggren, W.A., Kent, D.V., Swisher, C.C.S. III, Aubry, M.P., 1995. A revised Cenozoic geochronology and chronostratigraphy. In: Berggren, W.A., Kent, D.V., Hardenbol, J. (Eds.), Geochronology, Time Scales and Global Stratigraphic Correlations: A Unlithified Temporal Framework for an Historical Geology. Society of Economic and Paleontology Mineralogy Special Volume 54, pp. 129–260.

Bernet, K., Eberli, G.P., Gilli, A., 2000. Turbidite frequency and composition in the distal part of the Bahamas Transect. In: Swart, P.K., Eberli, G.P., Malone, M., Sarg, J.F. (Eds.), Proc. ODP, Sci. Results, 166. College Station, TX, pp. 45–60.

Betzler, C., Reijmer, J.J.G., Bernet, K., Eberli, G.P., Anselmetti, F.S., 1999. Sedimentary patterns and geometries of the Bahamian outer carbonate ramp (Miocene and lower Pliocene, Great Bahama Bank). Sedimentology 46, 1127–1145.

Blow, W.H., 1969. Late middle Eocene to Recent planktonic foraminiferal biostratigraphy. Proc. 1st Intl. Conf. Planktonic Microfossils, pp. 199–422.

Boardman, M.R., Neumann, A.C., 1984. Sources of periplatform carbonate: Northwest Providence Channel, Bahamas. J. Sediment. Petrol. 50, 1121–1148.

Bolli, H.M., Saunders, J.B., 1985. Oligocene to Holocene low latitude planktic foraminifera. In: Bolli, H.M., Saunders, J.B., Perch-Nielsen, K. (Eds.), Plankton Stratigraphy. Cambridge Earth Science Series, Cambridge University Press, Cambridge, pp. 155–262.

Cathles, L.M., Hallam, A., 1991. Stress-induced changes in plate density, Vail sequences, epeirogeny, and short-lived global sea level fluctuations. Tectonics 10, 659–671.

Chaisson, W.P., Pearson, P.N., 1997. Planktonic foraminifer biostratigraphy at ODP Site 925, western tropical Atlantic: the last 12 m.y. In: Curry, W.B., Shackleton, N.J., Richter, C. (Eds.), Proc. ODP, Sci. Results, 154. College Station, TX, pp. 3–31.

Cloetingh, S., 1986. Intraplate stresses: A new tectonic mechanism for fluctuations of relative sea level. Geology 14, 617–620.

Curry, W.B., Shackleton, N.J., Richter, C., 1995. Proc. ODP, Initial Reports, 154. College Station, TX.

Droxler, A.W., Schlager, W., 1985. Glacial versus interglacial sedimentation rates and turbidite frequency in the Bahamas. Geology 13, 799–802.

Droxler, A.W., Schlager, W., Whallon, C.C., 1983. Quaternary aragonite cycles and oxygen-isotope record in Bahamian carbonate ooze. Geology 11, 235–239.

Eberli, G.P., 1988. Physical properties of carbonate turbidite sequences surrounding the Bahamas – Implications for slope stability and fluid movements. In: Austin, J.A. Jr., Schlager, W. (Eds.), Proc. ODP, Sci. Results, 101, pp. 305–326.

Eberli G.P., Anselmetti, F.S., Kenter, J.A.M., McNeill, D.F., Melim, L.A., 2001. Calibration of seismic sequence stratigraphy with cores and logs. In: Ginsburg, R.N. (Ed.), The Bahamas Drilling Project. SEPM Special Publication 70, pp. 241–266.

Eberli, G.P., Ginsburg, R.N., 1987. Segmentation and coalescence of platforms, Tertiary, NW Great Bahama Bank. Geology 15, 75–79.

Eberli, G.P., Ginsburg, R.N., 1989. Cenozoic progradation of NW Great Bahamas Bank – A record of lateral platform growth and sea level fluctuations. In: Crevello, P.D. et al. (Eds.), Controls on Carbonate Platforms and Basin Evolution. SEPM Special Publication 44, pp. 339–355.

Eberli, G.P., Swart, P.K., Malone, M. et al., 1997. Proc. ODP, Initial Reports, 166. College Station, TX.

Eberli, G.P., Swart, P.K., McNeill, D.F., Kenter J.A.M., Anselmetti, F.S., Melim, L.A., Ginsburg R.N., 1997. A synopsis of the Bahamas Drilling Project: results from two deep core borings drilled on the Great Bahama Bank. In: Eberli, G.P., Swart, P.K., Malone, M. (Eds.), Proc. ODP, Initial Reports, 166. College Station, TX, pp. 23–42.

Frank, T.D., Bernet, K.H., 2000. Isotopic signature of burial diagenesis and primary lithologic contrasts in periplatform carbonates (Miocene, Great Bahama Bank). Sedimentology 47, 1256–1267.

Ginsburg, R.N., 2001. Subsurface Geology of a Prograding Carbonate Platform Margin, Great Bahama Bank. SEPM Special Publication 70, p. 272.

Glaser, K.S., Droxler, A.W., 1991. High production and highstand shedding from deeply submerged carbonate banks, northern Nicaragua Rise. J. Sediment. Petrol. 61, 128–142.

Grammer, G.M., Ginsburg, R.N., Harris, P.M., 1993. Timing of deposition, diagenesis, and failure of steep carbonate slopes in response to a high-amplitude/high-frequency fluctuation in sea level, Tongue of the Ocean, Bahamas. In: Loucks, R.G., Sarg, J.F. (Eds.), Carbonate Sequence Stratigraphy. American Association of Petroleum Geologists, Memoir 57, pp. 107–131.

Haq, B.U., Hardenbol, J., Vail, P.R., 1987. Chronology of fluctuating sea levels since the Triassic. Science 235, 1156–1167.

Kennett, J.P., Srinivasan, M.S., 1983. Neogene Planktonic Foraminifera. Hutchison Ross, Stroudsburg, PA.

Kenter, J.A.M., Ginsburg, R.N., Troelstra, S.R., 2001. The western Great Bahama Bank: sea-level-driven sedimentation patterns on the slope and margin. In: Ginsburg, R.N. (Ed.), Subsurface Geology of a Prograding Carbonate Platform Margin, Great Bahama Bank. SEPM Special Publication 70, pp. 61–100.

Kievman, C.M., 1996. Sea level effects on carbonate platform evolution: Plio-Pleistocene, northwestern Great Bahama Bank (Ph.D. thesis). University of Miami, Miami, FL.

Kievman, C.M., 1998. Match between late Pleistocene Great Bahama Bank and deep-sea oxygen isotope records of sea level. Geology 26, 635–638.

Kramer, P., Swart, P.K., De Carlo, E.H., Schovsbo, N.H., 2000. Overview of interstitial fluid and sediment geochemistry, sites 1003–1107 (Bahamas Transect). In: Swart, P.K., Eberli, G.P., Malone, M., Sarg, J.F. (Eds.), Proc. ODP, Sci. Results, 166. College Station, TX, pp. 179–195.

Kroon, D., Williams, T., Pirmez, C., Spezzaferri, T., Sato, T., Wright, J.D., 2000. Coupled Early Pliocene–Middle Miocene bio-cyclostratigraphy of Site 1006 reveals orbitally induced cyclicity patterns of Great Bahama Bank carbonate production. In: Swart, P.K., Eberli, G.P., Malone, M., Sarg, J.F. (Eds.), Proc. ODP, Sci. Results, 166. College Station, TX, pp. 155–166.

Leg 166 shipboard party, 1997. Leg 166-Synthesis. In: Eberli, G.P., Swart, P.K., Malone, M. (Eds.), Proc. ODP, Initial Reports, 166. College Station, TX, pp. 114–128.

Lidz, B.H., Brawlower, T.J., 1994. Microfossil biostratigraphy of prograding Neogene platform-margin carbonates, Bahamas: age constraints and alternatives. Mar. Micropaleontol. 23, 265–344.

Lidz, B.H., McNeill, D.F., 1995a. Deep-sea biostratigraphy of prograding platform margins (Neogene, Bahamas): Key evidence linked to depositional rhythm. Mar. Micropaleontol. 25, 87–125.

Lidz, B.H., McNeill, D.F., 1995b. Reworked Paleogene to early Neogene planktic foraminifera: implications of an intriguing distribution at a late Neogene prograding margin, Bahamas. Mar. Micropaleontol. 25, 221–268.

Martini, E., 1971. Standard Tertiary and Quaternary calcareous nannoplankton zonation. In: Farinacci, A. (Ed.), Proc. 1st International Planktonic Conference. Edit. Tecoscienza, Rome, pp. 739–785.

Mayer, L.A., 1979a. Deep sea carbonates: acoustic, physical, and stratigraphic properties. J. Sediment. Petrol. 49, 819–836.

Mayer, L.A., 1979b. The origin of fine scale acoustic stratig-

raphy in deep sea carbonates. J. Geophys. Res. 84, 6177–6184.
Mayer, L.A., Shipley, T.H., Winterer, E.L., 1986. Equatorial Pacific seismic reflectors as indicators of global oceanographic events. Nature 233, 761–764.
McNeill, D.F., Eberli, G.P., Lidz, B.H., Swart, P.K., Kenter, J.A.M., 2001. Chronostratigraphy of prograding carbonate platform margins: A record of dynamic slope sedimentation, Western Great Bahama Bank. In: Ginsburg, R.N. (Ed.), Subsurface Geology of a Prograding Carbonate Platform Margin, Great Bahama Bank. SEPM Special Publication 70, pp. 101–136.
Miall, A.D., 1986. Eustatic sea level changes interpreted from seismic stratigraphy. A critique of the methodology with particular reference to the North Sea Jurassic record. Am. Assoc. Petrol. Geol. Bull. 70, 131–137.
Payton, C.E., 1977. Seismic Stratigraphy – Applications to Hydrocarbon Exploration. American Association of Petroleum Geologists Memoir 26, p. 516.
Pitman, W., Golovchenko, X., 1983. The effect of sea-level change on the shelf-edge and slope of passive margins. SEPM Special Publication 33, pp. 41–58.
Reijmer, J.J.G., Schlager, W., Droxler, A.W., 1988. Site 632: Pliocene–Pleistocene sedimentation in a Bahamian basin. Proc. ODP, Sci. Results, 101, pp. 213–220.
Rendle, R.H., Reijmer, J.J.G., 2002. Evolutionary slope development of the western, leeward margin of Great Bahama Bank during the Quaternary. Mar. Geol. 185, S0025-3227(01)00294-8.
Rendle, R.H., Reijmer, J.J.G., Kroon, D., Henderson, G.M., 2000. Mineralogy and sedimentology of Pleistocene to Holocene on the leeward margin of Great Bahama Bank. In: Swart, P.K., Eberli, G.P., Malone, M., Sarg, J.F. (Eds.), Proc. ODP, Sci. Results, 166. College Station, TX, pp. 61–76.
Rudolph, K.W., Schlager, W., Biddle, K.T., 1989. Seismic models of a carbonate foreslope-to-basin transition, Picco di Vallandro, Dolomite Alps, northern Italy. Geology 17, 453–456.
Schlager, W., 1992. Sedimentology and sequence stratigraphy of reefs and carbonate platforms. American Association of Petroleum Geologists Continuing Education Course Note Series 34, p. 71.
Schlager, W., Reijmer, J.J.G., Droxler, A.W., 1994. Highstand shedding of carbonate platforms. J. Sediment. Res. B64, 270–281.
Stafleu, J., Everts, A.J.W., Kenter, J.A.M., 1994. Seismic models of a prograding carbonate platform: Vercors, SE France. Mar. Petrol. Geol. 11, 514–517.
Stafleu, J., Sonnenfeld, M.D., 1994. Seismic models of a shelf-margin depositional sequence: Upper San Andres Formation, Last Chance Canyon, New Mexico. J. Sediment. Res. B64, 481–499.
Summerhayes, C.P., 1986. Sea-level curves based on seismic stratigraphy: their chronostratigraphic significance. Palaeogeogr. Palaeoecol. Palaeoclimatol. 57, 27–42.
Swart, P.K., Eberli, G.P., Malone, M., Sarg, J.F., 2000. Proc. ODP, Sci. Results, 166. College Station, TX.
Swart, P.K., Elderfield, H., Beets, K., 2001. The $^{87}Sr/^{86}Sr$ ratios of carbonates, phosphorites, and fluids collected during the Bahama Drilling Project cores Clino and Unda: Implications for dating and diagenesis. In: Ginsburg, R.N. (Ed.), Subsurface Geology of a Prograding Carbonate Platform Margin, Great Bahama Bank. SEPM Special Publication 70, pp. 175–186.
Tipper, J.C., 1993. Do seismic reflections necessarily have chronostratigraphic significance? Geol. Mag. 130, 47–55.
Vail, P.R., Mitchum, R.M. Jr., Thomson, S., 1977. Seismic stratigraphy and global changes of sea level. In: Payton, C.E. (Ed.), Seismic Stratigraphy – Applications to Hydrocarbon Exploration. American Association of Petroleum Geologists Memoir 26, pp. 49–212.
Vail, P.R., Todd, A.G., Sangree, J.B., 1977. Chronostratigraphic significance of seismic reflections. In: Payton, C.E. (Ed.), Seismic Stratigraphy – Applications to Hydrocarbon Exploration. American Association of Petroleum Geologists Memoir 26, pp. 99–116.
Watkins, J.S., Drake, C.L., 1982. Studies in Continental Margin Geology. American Association of Petroleum Geologists Memoir 34.
Weimer, P., Davis, T.L., 1996. Applications of 3-D seismic data to exploration and production. AAPG Studies in Geology No. 42 and SEG Geophysical Development Series No. 5, p. 270.
Westphal, H., 1998. Carbonate platform slopes – a record of changing conditions. Lecture Notes in Earth Sciences 75, Springer Verlag, Berlin.
Westphal, H., Reijmer, J.J.G., Head, M.J., 1999. Sedimentary input and diagenesis on a carbonate slope (Bahamas): Response to morphology evolution of the carbonate platform and sea level fluctuations. In: Harris, P.M., Saller, A.H., Simo, T. (Eds.), Advances in Carbonate Sequence Stratigraphy – Application to Reservoirs, Outcrops, and Models. SEPM Special Publication 63, pp. 247–274.
Wilber, R.J., Milliman, J.D., Halley, R.B., 1990. Accumulation of Holocene banktop sediment on the western margin of Great Bahama Bank: Rapid progradation of a carbonate megabank. Geology 18, 970–974.
Williams, T., Kroon, D., Spezzaferri, S., 2002. Middle-Upper Miocene cyclostratigraphy of downhole logs and short to long term astronomical cycles in carbonate production of the Great Bahama Bank. Mar. Geol. 185, S0025-3227(01)00291-2.
Wright, J.D., Kroon, D., 2000. Planktonic foraminiferal biostratigraphy of Leg 166. In: Swart, P.K., Eberli, G.P., Malone, M., Sarg, J.F. (Eds.), Proc. ODP, Sci. Results, 166. College Station, TX, pp. 3–12.